Physics of Wave Processes and Radio Systems
2023, vol. 26, no. 1, pp. 38–48

DOI 10.18469/1810-3189.2023.26.1.38-48

Received 29 November 2022
Accepted 30 December 2022

Mathematical models of spheroidal spiral-frame radiating structures

Dmitry P. Tabakov, Ruslan M. Valiullin

Povolzhskiy State University of Telecommunications and Informatics
23, L. Tolstoy Street,
Samara, 443010, Russia

Abstract – The article considers mathematical models of two spheroidal spiral-frame emitters, built on the basis of a general approach involving the use of an integral representation electromagnetic field. The internal problem of electrodynamics is reduced to a system of Fredholm integral equations of the 1st kind. The resulting system was solved by the method of moments with piecewise constant basis functions and delta functions as test functions. In this case, the local linearization of the generating conductors of the structures under consideration was carried out. The dependences of current distributions, input resistance, and radiation characteristics of structures on frequency have been studied. It is shown that standing, traveling, and mixed current waves can exist in the structures under consideration. The current regime is determined by the wave sizes and the geometry of the structures and determines the behavior of the wave resistance in the frequency range. Despite the similar geometry, the characteristics of the considered structures have certain differences.

Keywords – helical antennas; loop antennas; integral representation electromagnetic field; thin-wire approximation; radiation pattern; input impedance.

Introduction

Helical antennas (HAs) represent a wide class of radiating structures, whose geometry and characteristics meet predetermined and diverse requirements. The main advantages of HAs include the ability to achieve a wide operating frequency band, good radiation directivity characteristics, the ability to electrically control the polarization characteristics of the radiation, and various shapes of emitting elements. Subject to the principle of angles and complementarity, frequency-independent variants of HA are implemented, the overlap coefficient of which reaches several tens of units [1]. HAs are used in antenna technology as self-sufficient radiating structures, as feeds for mirror antennas, in phased antenna arrays, to construct slow-wave systems, and in other elements of microwave devices [2].

Currently, interest in spiral elements is also associated with the development of the theory of metamaterials [3], while chiral structures can be considered a special case [4]. The introduction of conductive particles of various configurations (in this case, spiral particles) into the source material changes its electrodynamic properties. Such structures can be used as frequency-selective elements in polarization converters as low-reflective coatings and microwave energy concentrators. Naturally, the construction of the abovementioned structures requires the presence of mathematical models (MMs) of their basic elements, which in this case are spiral elements, generally described by sufficiently numerous parameters. Currently, phenomenological equations operating with the chirality parameter χ are used to study chiral structures [4–6]. The value and sign of χ depend on the wavelength and the type of basic elements. χ is determined using approximate methods. However, the use of phenomenological equations has important limitations associated with the relative position and wave sizes of the elements forming the structure. In general, for metamaterials, the practice of description based on effective dielectric and magnetic permeabilities, which generally have a tensor form, is considered acceptable. Approximate and rigorous approaches are used to analyze the helical structures. Within the framework of approximate approaches, the original emitter is replaced with a simplified equivalent (e.g., an array of ring elements, a single ring element, or an anisotropic conductive model). [2; 7]). Moreover, these approaches can be considered most adequate when applied to regular spiral structures. When studying irregular structures, the principle of local equivalence is used, further reducing the correspondence of the approximate solution to the exact solution of the problem.

The problem with the currently existing exact methods used in computer-aided design systems (CST MWS, FEKO, and HFSS) is the high requirements for computing resources, which are a consequence of their versatility, as well as the numerical nature of the results obtained, which cannot always be interpreted correctly. Therefore, the construction of rigorous and computationally efficient MMs of

✉ illuminator84@yandex.ru (*Dmitry P. Tabakov*)

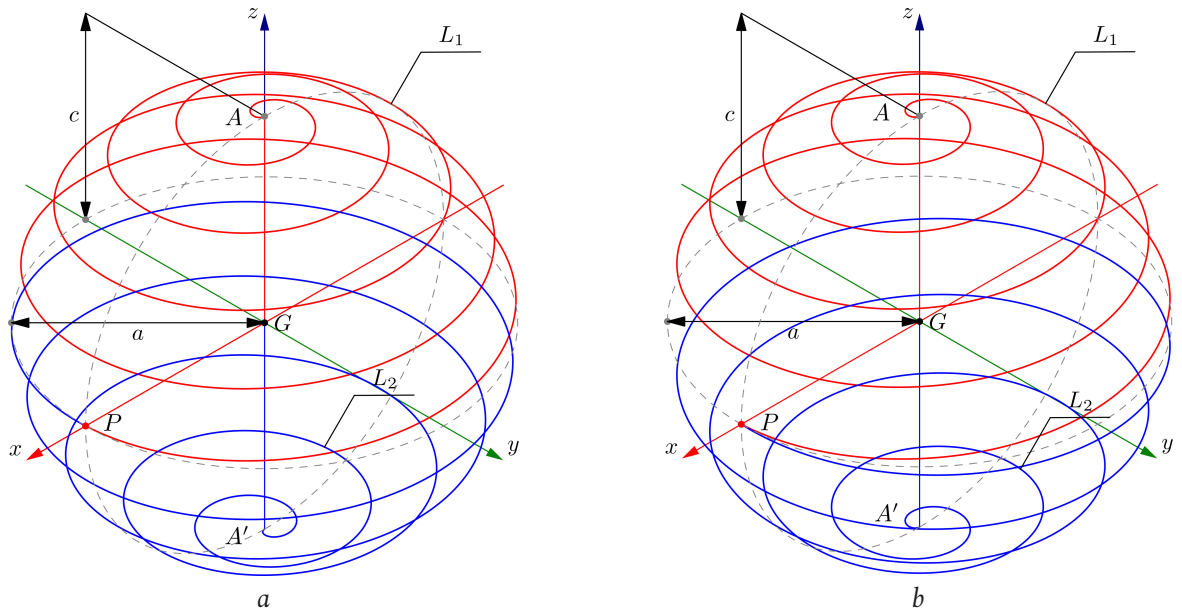

Fig. 1. Geometry of the structures under study: without a break (*a*) and with a break (*b*)
Рис. 1. Геометрия исследуемых структур: без излома (*а*) и с изломом (*б*)

spiral elements and structures using these elements as their basis is a relevant task.

The most accurate MMs are constructed on the basis of integral equations (IEs) of various types [8–11]. The most widely used MMs are in the form of Fredholm IE systems of the first kind, obtained using the thin-wire (TW) approximation [12]. Herein, the complete MM of the structure under consideration must comprise the solution of exterior (determination of EMF [electromagnetic field] at any point in space) and interior (determination of current functions from boundary conditions on the elements of the structure) electrodynamic problems. The IE system represents a solution to only an internal problem. Therefore, the MM should be constructed on the basis of the corresponding integral representation of the EMF (EMF IR), which maintains a continuous relationship between the current functions and their EMF generated at any point in space.

In [13], based on TW EMF IR, the construction of MMs of cylindrical spiral elements of two types (conventional and combined) was performed. The problem of diffraction of these elements has been solved. It was revealed that the interior structure of the element considerably influences the scattered field characteristics. Thus, on a combined spiral element in a rather wide frequency range, the effect of orthogonal scattering occurs when the angle between the wave vectors of the primary and scattered electromagnetic waves is near 90°.

In [14], an ellipsoidal spiral particle was discussed, in which the MM was also constructed on the basis of the TW EMF IR. At the same time, a detailed analysis of the solution to the spectral problem was performed, which consisted of determining the behavior of the eigenfunctions and eigenvalues of the integral operator in the frequency band. It was demonstrated that the solution to the interior problem as a whole is determined by the eigenfunctions that have the smallest absolute value of the associated eigenvalues.

In this article, the MMs of two types of spiral-frame emitters are proposed, for which a numerical solution of the interior problem is studied in the frequency range. The radiation characteristics and input resistance are then determined. These emitters can be used as self-sufficient antennas or as a part of more complex antenna systems.

1. Physical models and geometry of the radiating structures

The geometry of the emitters is shown in Fig. 1. Both structures include a straight axial conductor *A'A* located along the axis O_z and a pair of spiral conductors *AP* and *A'P* connected to each other at a point *P* and at the corresponding ends *A* and *A'* of the axial conductor. The structure presented in Fig. 1*a* contains a regular ellipsoidal helix (hereinafter referred to as A-helix). The structure presented in Fig. 1*b* comprises a spiral with a kink, and its lower part is a mirror image of the upper part relative to the plane *XOY*.

The structure conductors have the same radius, equal to $\varepsilon = \lambda$, where λ is the radiation wavelength. At point *G*, the axial conductor has a gap of length

$2b = \lambda$, which comprises an external field source (EMF generator). The tangential component of the external field on the conductors $E^{(\text{in})}$ is zero everywhere, except the discontinuity region, where it is equal to $U/(2b)$, where U is the EMF generator voltage. Under the influence of an external field, a distribution of electric current $I(l)$ arises in conductors, the type of which must be determined when solving an interior electrodynamic problem. Because $2b = \lambda$, the function $I(l)$ is continuous in the discontinuity region. In addition, when constructing the MM, we assume that the conductors have infinitely large conductivity.

The generalized parametric equation of the spiral generatrix L_s has the form:

$$L_s: \quad \mathbf{r}_l(\varphi) = a\cos(\varsigma\varphi)\cos\varphi\hat{\mathbf{x}} + \\ + af(\varphi)\cos(\varsigma\varphi)\sin\varphi\hat{\mathbf{y}} + c\sin(\varsigma\varphi)\hat{\mathbf{z}}, \\ \varsigma = 1/(2N_l), \varphi \in [-1;1]\cdot\pi N_l. \tag{1}$$

Here, a is the spheroid radius, and c is its semiaxis; φ is a parameter on the generatrix (essentially the azimuth of the cylindrical coordinate system), and N_l is the number of helical turns. For A-helix, $f(\varphi) = 1$, and for B-helix, $f(\varphi) = \operatorname{sgn}(\varphi)$, where $\operatorname{sgn}(\varphi)$ is the sign function. For the transition in Eq. (1) from a parameter φ to a natural parameter l, it is necessary to define the function $\varphi = \varphi(l)$ inverse to the function:

$$l(\varphi) = \int_0^{\varphi} \left|\frac{\partial \mathbf{r}_l(\varphi')}{\partial\varphi}\right| d\varphi', \tag{2}$$

and substitute it into Eq. (1). In this case, this problem can only be solved numerically using the inverse interpolation method [15]. The equation for the axial conductor L_v is written directly in the natural parameter l:

$$L_v: \mathbf{r}_v(l) = l\hat{\mathbf{z}}, \quad l \in [-c;c]. \tag{3}$$

2. MMs of the radiating structures

To construct MMs of emitters in the previously considered formulation, an EMF IR is used [13]:

$$\mathbf{F}(\mathbf{r}) = \sum_j \mathbf{F}(\mathbf{r};\mathbf{r}_j,I_j); \quad F \equiv E,H, \tag{4}$$

Here,

$$\mathbf{F}(\mathbf{r};\mathbf{r}_j,I_j) = \int_{L_j} I_j(l')\mathbf{K}_a^F(\mathbf{r},\mathbf{r}_j(l'))dl', \quad F \equiv E,H \tag{5}$$

is the EMF IR from the current $I_j(l)$, localized on the TWS generatrix L_j,

$$\mathbf{K}_a^E(\mathbf{r},\mathbf{r}_j(l')) = \frac{W_m}{ik}\left(\hat{\mathbf{l}}_j(l')k^2 G_a(\mathbf{r},\mathbf{r}_j(l')) + \right.$$

$$\left. + \frac{\partial}{\partial l'}\left((\mathbf{r}-\mathbf{r}_j(l'))B_a(\mathbf{r},\mathbf{r}_j(l'))\right)\right);$$

$$\mathbf{K}_a^H(\mathbf{r},\mathbf{r}_j(l')) = \left((\mathbf{r}-\mathbf{r}_j(l'))\times\hat{\mathbf{l}}_j(l')\right)B_a(\mathbf{r},\mathbf{r}_j(l')),$$

are the kernels of the EMF IR; $\hat{\mathbf{l}}_j(l) = d\mathbf{r}_j(l)/dl$ is the tangent unit on the generatrix L_j; W_m is the wave impedance of the medium, and k is its wave number;

$$B = -\frac{ikR+1}{R^2}G, \quad G = \frac{\exp(-ikR)}{4\pi R},$$

$G(R)$ is Green's function defined for free space; $R(\mathbf{r},\mathbf{r}') = |\mathbf{r}-\mathbf{r}'|$ is the distance between the source and observation points;

$$F_a(\mathbf{r},\mathbf{r}_j(l')) = F(R_a(\mathbf{r},\mathbf{r}_j(l'))), \quad F \equiv G,B$$

are kernel components, and

$$R_a(\mathbf{r},\mathbf{r}_j(l')) = \sqrt{|\mathbf{r}-\mathbf{r}_j(l')|^2 + \varepsilon^2}$$

is the distance between the source and observation points, regularized by a small parameter ε, whose function is performed by the radius of the conductors. In our case, Eq. (4) involves a pair of conductors $L_1 = L_v$ and $L_2 = L_s$.

The integral representation of the EMF of Eq. (4) contains current functions $I_j(l)$, to be determined. This can be achieved by applying a boundary condition on the surface of the conductors. Because $\varepsilon = \lambda$, the boundary condition can be weakened by moving from the surface of the conductors to their generatrices. Thus, we obtain the following:

$$\hat{\mathbf{l}}(\mathbf{r}(l))\cdot\left(\mathbf{E}^{(in)}(\mathbf{r}(l)) + \mathbf{E}(\mathbf{r}(l))\right) = 0. \tag{6}$$

The result of applying the presented boundary equation to the EMF IR is a system of IEs of the form:

$$-\hat{\mathbf{l}}(\mathbf{r}_i)\cdot\mathbf{E}^{(in)}(\mathbf{r}_i) = \hat{\mathbf{l}}(\mathbf{r}_i)\cdot\sum_j \mathbf{E}(\mathbf{r}_i;\mathbf{r}_j,I_j); \tag{7}$$

$i,j = 1,\ldots,N.$

The given IE system is classified as a Fredholm IE system of the first kind [16]. Let us discretize Eq. (4) by replacing the generators with kinked curves:

$$L_j \to L_j^{\{N_j\}}: \mathbf{r}_{j,1},\mathbf{r}_{j,2},\ldots,\mathbf{r}_{j,N+1}, \tag{8}$$

where $N_j + 1$ is the number of nodes of the kinked curve, and j is the index of the conductor. For each kinked curve, we can determine the following equation of the (j,k_j)-segment:

$$\mathbf{r}_{j,k_j} = \overset{*}{\mathbf{r}}_{j,k_j} + \hat{\mathbf{l}}^*_{j,k_j} l, \quad l \in [-\Delta_j/2;\Delta_j/2], \tag{9}$$

Here,

$$\overset{*}{\mathbf{r}}_{j,k_j} = \frac{\mathbf{r}_{j,k_j+1} + \mathbf{r}_{j,k_j+1}}{2}, \tag{10}$$

$$\hat{\mathbf{l}}^*_{j,k_j} = \frac{\mathbf{r}_{j,k_j+1} - \mathbf{r}_{j,k_j+1}}{\Delta_j}, \quad \Delta_j = |\mathbf{r}_{j,k_j+1} - \mathbf{r}_{j,k_j+1}|$$

is the center of the segment, the unit tangent vector on the segment, and its length, respectively, $k_j = 1,\dots N_j + 1$. Let I_{j,k_j} be the complex amplitude of the current (j,k_j)-segment. Then, for the discretize generatrices based on Eq. (4), we obtain the EMF IR of a set of *N* emitters having segmented generatrices:

$$\mathbf{F}(\mathbf{r}) = \sum_{j=1}^{N}\sum_{k_j=1}^{N_j} I_{j,k_j} \int_{-\Delta_j/2}^{\Delta_j/2} \mathbf{K}_a^F(\mathbf{r}, \mathbf{r}_{j,k_j}(l'))dl', \quad F \equiv E, H. \qquad (11)$$

Use of Eq. (11) presupposes knowledge of unknown current amplitudes I_{j,k_j}. Within the chosen method for solving the IE system, a boundary condition of the Eq. (6) type must be fulfilled at the centers of the segments. Consequently, we have the following SLAE (system of linear algebraic equations):

$$-\hat{\mathbf{l}}_{i,k_i}^{*}\mathbf{E}^{(\text{in})}(\mathbf{r}) = \sum_{j=1}^{N}\sum_{k_j=1}^{N_j} I_{j,k_j} \int_{-\Delta_j/2}^{\Delta_j/2} \hat{\mathbf{l}}_{i,k_i}^{*} \cdot \mathbf{K}_a^E(\mathbf{r}, \mathbf{r}_{j,k_j}(l'))dl', \quad (12)$$

$i = 1,\dots,N, \quad k_i = 1,\dots,N_i.$

If the condition is met that

$$2\varepsilon \le \Delta_j \le 12\varepsilon \qquad (13)$$

for all *j* values, a stable solution of the SLAE is obtained [12]. The reliability of the results obtained on the basis of Eq. (11) and Eq. (12) is confirmed in [17].

3. Results of the numerical modeling

During numerical modeling, A- and B-helices were studied, the geometry of which was determined by the following parameters: $a/c = 1/4,\ 1/2,\ 3/4$, and 1; the number of segments of the spiral element in the indicated cases was equal to 200, 400, 600, and 800, respectively; and the number of segments of the axial conductor was 80 for all a/c values. The number of turns of the spiral element was equal to five, and the ratio of the radius of the conductor ε to the semiaxis *c* was $\varepsilon/c = 3/1000$. The specified choice of geometric parameters satisfies the condition of Eq. (13), the implementation of which provides a correct solution to the interior problem. The doubled semiaxis *c* of the structures, which determines their height, was chosen as the main parameter normalized to the wavelength λ.

Fig. 2 presents the results of calculating the amplitude current distributions on the conductor *AP* of both structures for various ratios $2c/\lambda$ at $a/c = 1/2$. The value $2c/\lambda$ is indicated directly in the figures. According to the figure, at $2c/\lambda < 0{,}5$ a standing current wave regime is established in the spiral conductors, and the distributions for the A- and B-helices have several differences. This regime emerges because radiation losses at distances commensurate with the wavelength are quite small. Consequently, in a spiral conductor, there is a pair of counterpropagating traveling waves with a practically unchanged amplitude. Their sum represents a standing wave, which we can note in this figure at $2c/\lambda = 0{,}05$, 0,25, and 0,5. At $2c/\lambda = 0{,}6$, a mixed current wave mode is established in the spiral; counterpropagating waves have the greatest amplitude difference on the spiral near points *A* and *A*', and the smallest difference is at point *P*. Therefore, the standing current wave mode remains near point *P*. It is quite reasonable to state that for the indicated ratio $2c/\lambda = 0{,}6$, traveling and standing current waves make a commensurate contribution to the total field created by the structures under consideration, but the traveling waves of the A-helix lose energy more intensely than those of the B-helix; thus, differences in the calculation results for the structures under consideration become more noticeable. At $2c/\lambda = 0{,}75$ and 1,0, radiation is created predominantly by traveling waves, whose amplitude decreases considerably as they approach point *P*. The amplitude of standing waves in the A-helix near points *A* and *A*' is noticeably higher, but in general, the current distributions are approximately identical.

Figs. 3–6 show the results of calculating the input resistance of the structures under consideration for four ratios a/c. In terms of the input resistance for the structures under consideration, two regions can be conventionally distinguished: the low-frequency (LF) and high-frequency (HF) regions. In the LF region (Fig. 3, 4), in the current distribution along the conductors, standing waves are predominant, which forms the resonant nature of the dependence of the input resistance on frequency. The quality factor of the resonances directly depends on the degree of dominance of standing waves. In addition, as is seen from Figs. 3 and 4, it has an inverse dependence on the ratio a/c. In general, the dependence of the input resistance on frequency is very similar for A- and B-helixes in the LF region.

In the HF region, the dependence of the input resistance on frequency at $a/c > 0{,}5$ is smoother (Fig. 5, 6). The uniformity of the input resistance is noticeably higher for the B-helix than for the A-helix. According to Fig. 5, for an A-helix with the considered number of turns, the deviation of the input resistance from the average value is minimal at an optimal value of a/c (in this case $a/c = 0{,}5$). In the HF region, the input resistance has a capacitive com-

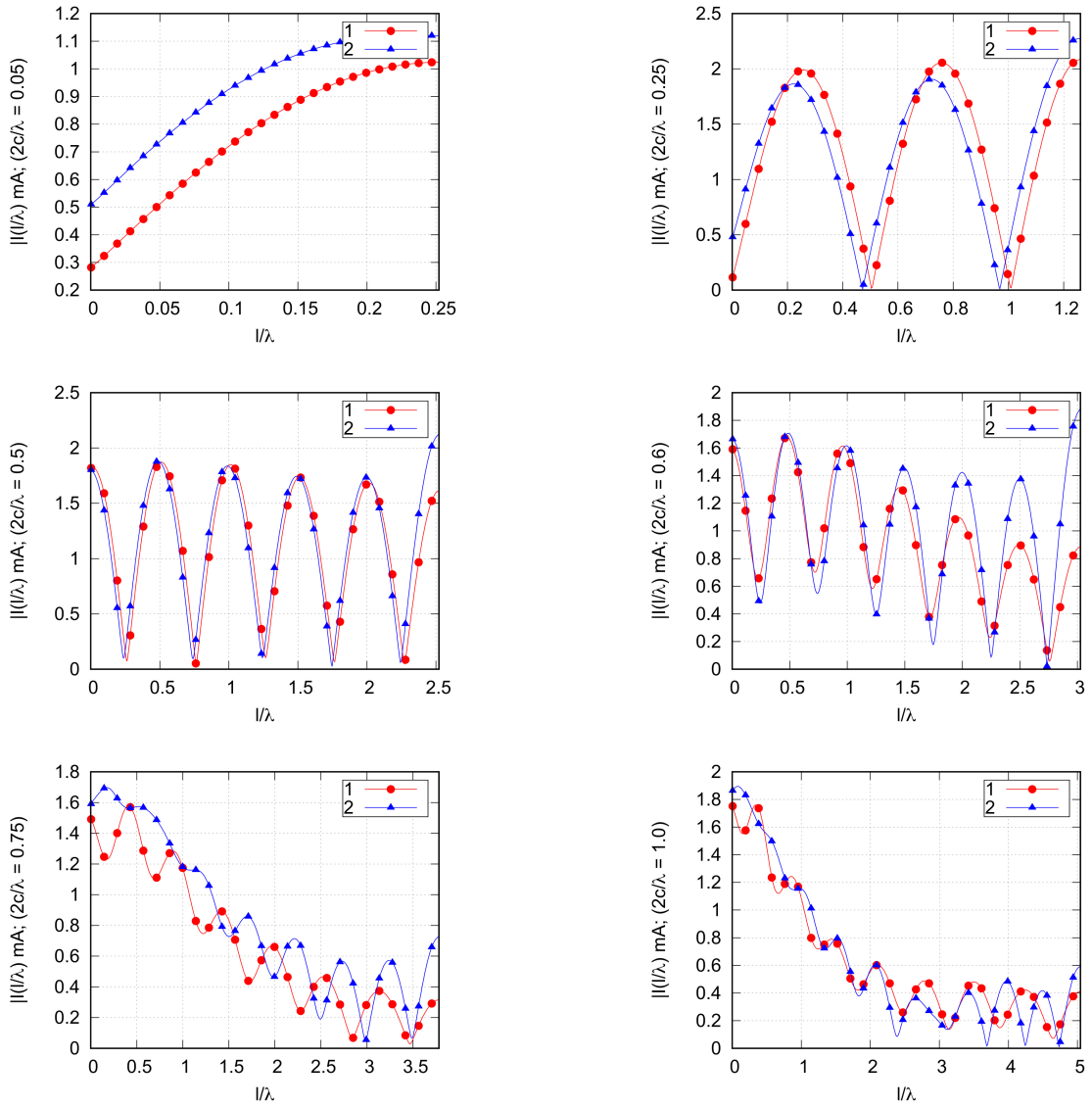

Fig. 2. Comparison of the amplitude distributions of the current on the conductor AP of the A-helix (curve 1) and B-helix (curve 2) at different values $2c/\lambda$; $a/c = 1/2$

Рис. 2. Сравнение амплитудных распределений тока на проводнике AP А-спирали (кривая 1) и Б-спирали (кривая 2) при различных значениях $2c/\lambda$; $a/c = 1/2$

ponent in the structures under consideration. With the lowest a/c value considered equal to $1/4$, the frequency dependence of the input resistance is in many ways reminiscent of a similar dependence for a symmetrical electric dipole.

Fig. 7 presents a comparison of the normalized amplitude directional patterns (DPs) of the considered emitters in the meridian plane, calculated at different ratios of $2c/\lambda$ and a fixed value $a/c = 1/2$. At $2c/\lambda < 0{,}25$, the DP is toroidal, repeating a similar DP of a symmetrical dipole. This result is obtained because the transverse size of the emitters is much smaller than the radiation wavelength. It is also seen that the spiral conductor structure does not substantially affect the radiation characteristics, and the DP of the A- and B-helices coincides with the graphical accuracy. A further increase in $2c/\lambda$ to 0,5 leads to the disappearance of radiation zeros toward the $A'A$ axis. With $2c/\lambda > 0{,}6$, the DP becomes near spheroidal. In this case, the differences in the DP of the A- and B-helices also increase.

Conclusion

This study considers two variants of spheroidal spiral-frame emitters (A-helix and B-helix). The emitters differ in the internal structure of the spiral elements. Note that HAs, which have a geometry near that of the emitters considered, are widely used in practice. MMs of emitters are proposed and constructed on the basis of an integral representation of the electromagnetic field recorded in the TW approximation. These MMs allow for a quantitative assessment of the

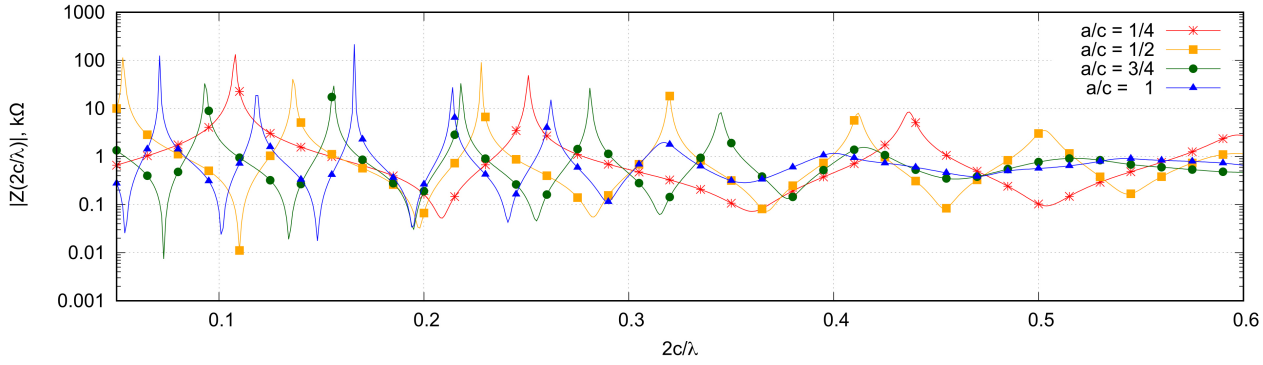

a

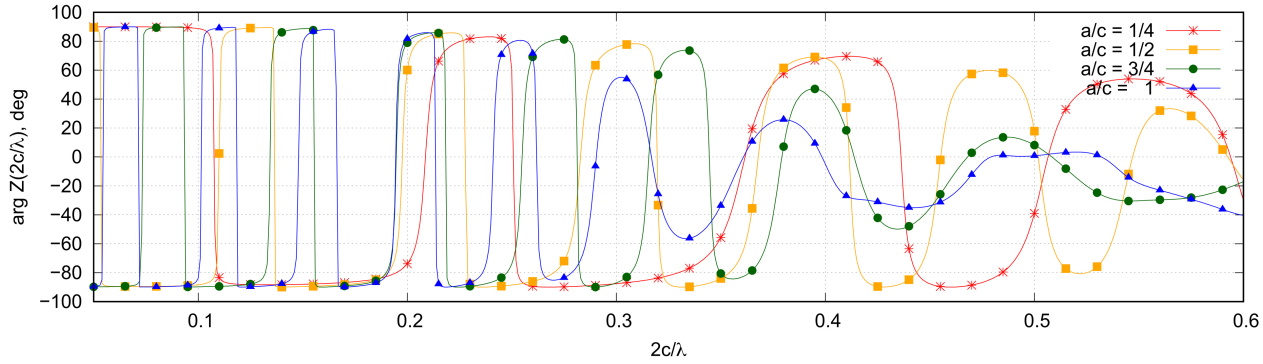

b

Fig. 3. Dependence of the amplitude (*a*) and phase (*b*) of the input resistance on the ratio $2c/\lambda$ for the A-helix; $2c/\lambda \in [0,05;0,6]$
Рис. 3. Зависимость амплитуды (*а*) и фазы (*б*) входного сопротивления от отношения $2c/\lambda$ для А-спирали; $2c/\lambda \in [0,05;0,6]$

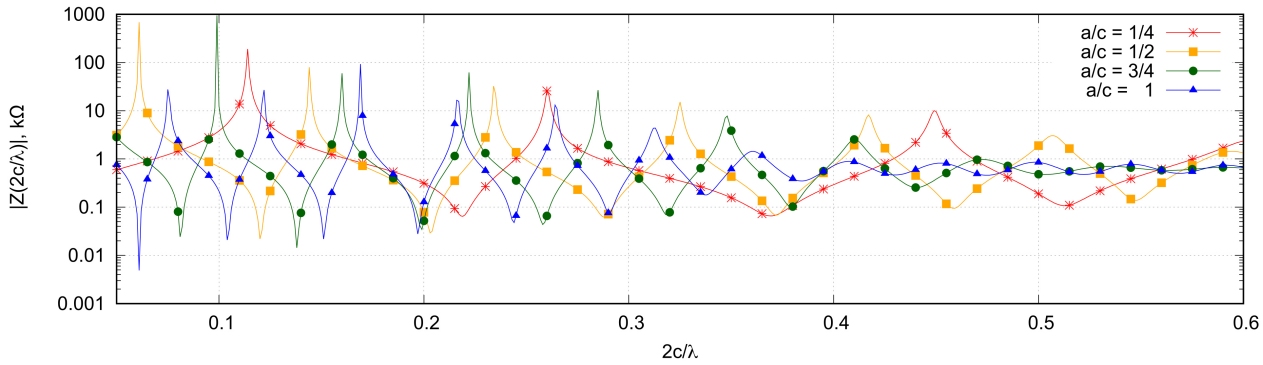

a

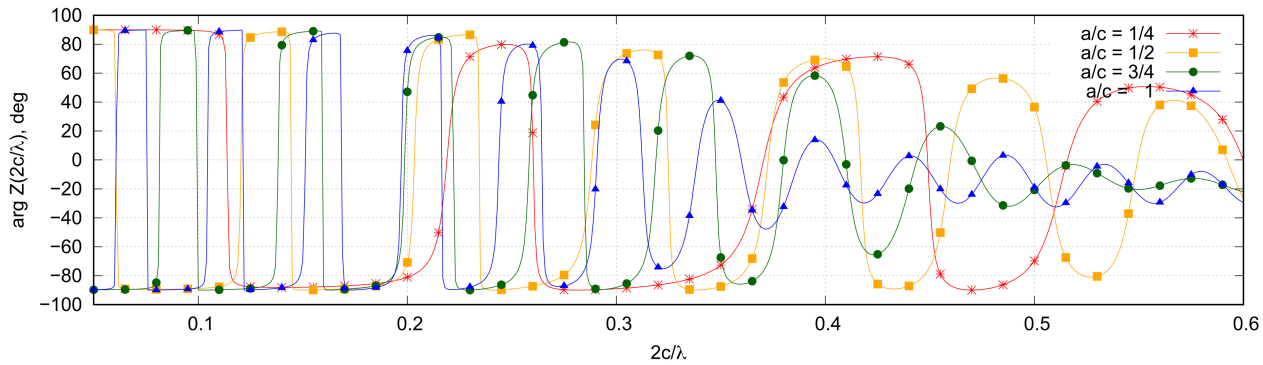

b

Fig. 4. Dependence of the amplitude (*a*) and phase (*b*) of the input resistance on the ratio $2c/\lambda$ for the B-helix; $2c/\lambda \in [0,05;0,6]$
Рис. 4. Зависимость амплитуды (*а*) и фазы (*б*) входного сопротивления от отношения $2c/\lambda$ для Б-спирали; $2c/\lambda \in [0,05;0,6]$

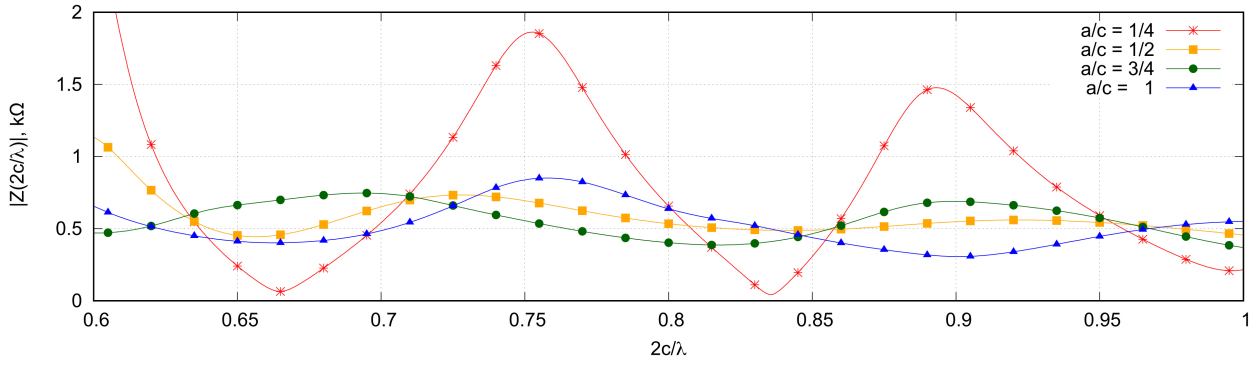

a

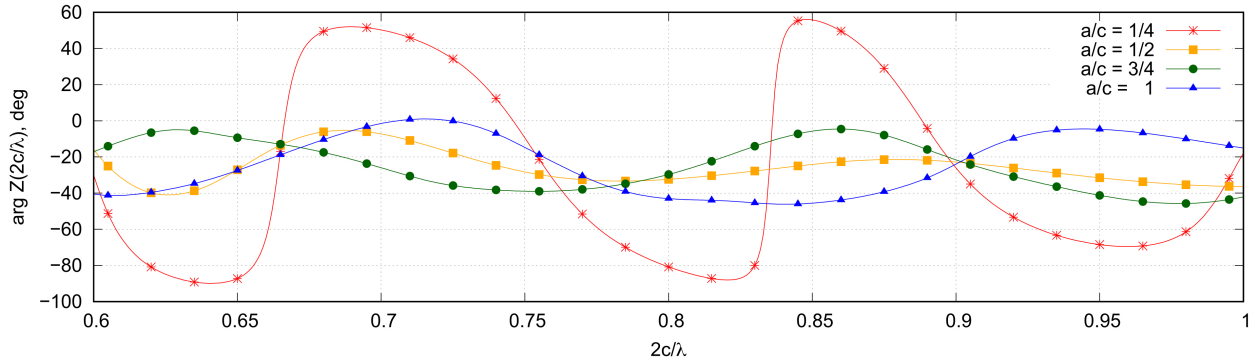

b

Fig. 5. Dependence of the amplitude (*a*) and phase (*b*) of the input resistance on the ratio $2c/\lambda$ for the A-helix; $2c/\lambda \in [0,6;1,0]$
Рис. 5. Зависимость амплитуды (*а*) и фазы (*б*) входного сопротивления от отношения $2c/\lambda$ для А-спирали; $2c/\lambda \in [0,6;1,0]$

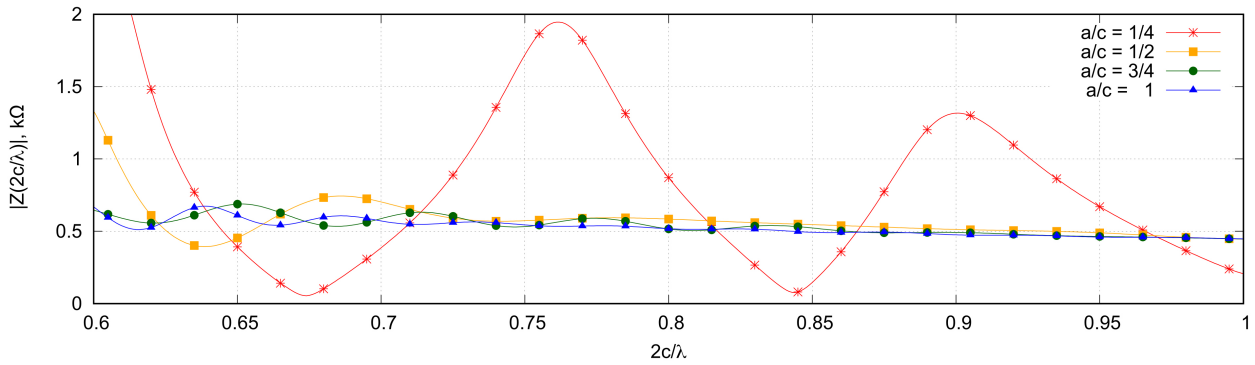

a

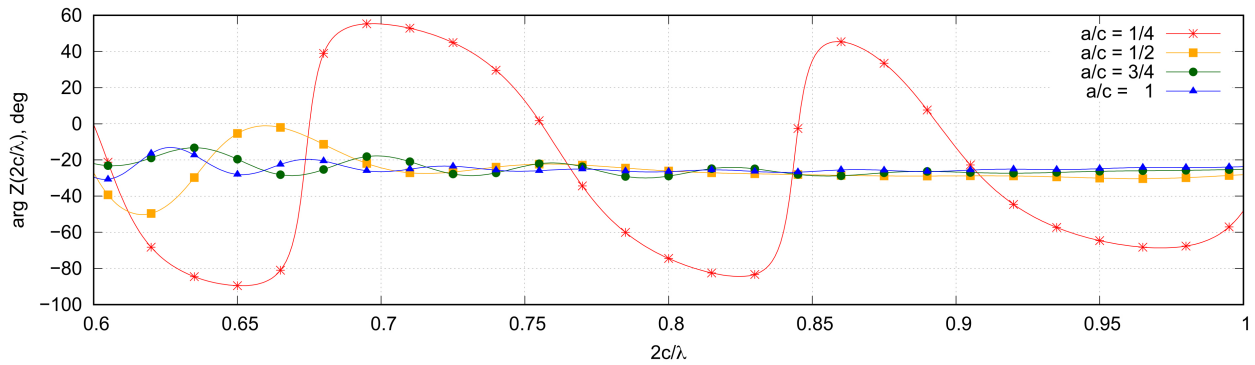

b

Fig. 6. Dependence of the amplitude (*a*) and phase (*b*) of the input resistance on the ratio $2c/\lambda$ for the B-helix; $2c/\lambda \in [0,6;1,0]$
Рис. 6. Зависимость амплитуды (*а*) и фазы (*б*) входного сопротивления от отношения $2c/\lambda$ для Б-спирали; $2c/\lambda \in [0,6;1,0]$

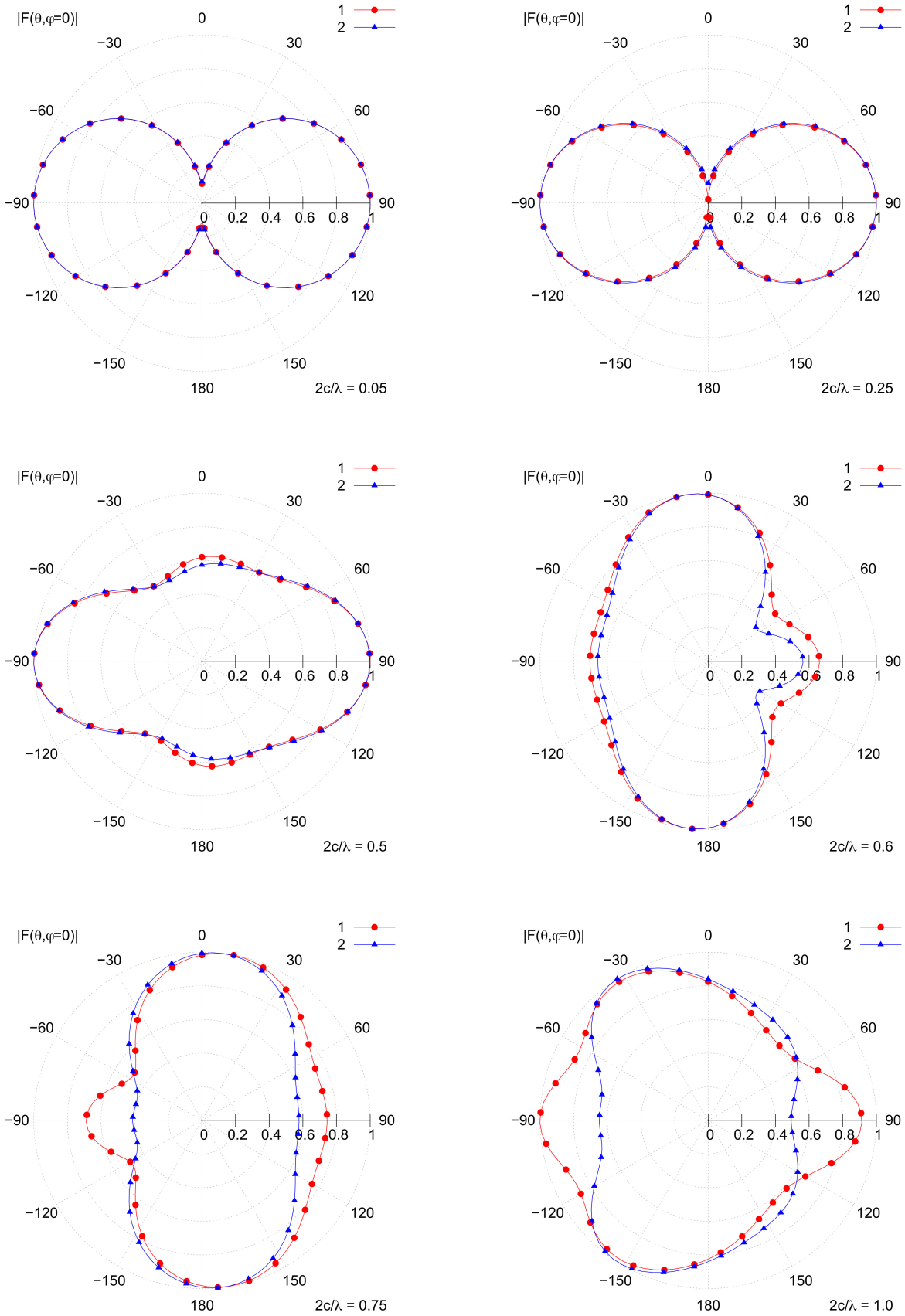

Fig. 7. Comparison of the normalized amplitude radiation patterns of the A-helix (curve 1) and B-helix (curve 2) at different values $2c/\lambda$
Рис. 7. Сравнение нормированных амплитудных диаграмм направленности А-спирали (кривая 1) и Б-спирали (кривая 2) при различных значениях $2c/\lambda$

electrodynamic parameters of the structures under consideration. The interior problem is described as a system of Fredholm IEs of the first kind. A method for reducing it to a SLAE presented with respect to unknown values of complex current amplitudes on segments is presented, and a condition is given for correctly implementing this procedure.

Based on the models presented, numerical solutions were obtained for the interior and exterior electrodynamic problems. For some ratios a/c in the range of values $2c/\lambda$, the current distributions, input resistance, and normalized radiation patterns were calculated. Physical interpretation is given to the results obtained. It is shown that in the structures considered, depending on the ratio $2c/\lambda$, the regime of a standing, traveling, or mixed current wave can be implemented. The standing wave mode occurs at small $2c/\lambda$, and the traveling wave mode is characteristic of $2c/\lambda > 3/4$. Analysis of the dependence of the input resistance on $2c/\lambda$ showed a close relationship between the current mode and the behavior of the input resistance. In addition, in the process of analyzing the results of the input resistance, it was established that the B-helix has greater uniformity of the input resistance at $2c/\lambda > 0,6$, and for the A-helix, minimum unevenness is achieved at an optimal ratio a/c. An analysis of the radiation characteristics showed that at small ratios of $2c/\lambda$ the normalized DP coincides in shape with the DPs of a symmetrical electric dipole; with an increase in $2c/\lambda$, the DP becomes near ellipsoidal. In the future, we plan to increase the computational efficiency of the proposed models using optimal systems of projection functions and analyze in more detail the numerical results for various ratios of the geometric parameters of the structures.

References

1. Ramsey V. *Frequency Independent Antennas*. Moscow: Mir, 1968, 176 p. (In Russ.)
2. Drabkin A.L., Zuzenko V.L., Kislov A.G. *Antenna-Feeder Devices*. 2nd ed., add. and reworked. Moscow: Sov. radio, 1974, 536 p. (In Russ.)
3. *Physical Encyclopedic Dictionary*. Ed. by A.M. Prokhorov. Moscow: Bol'shaya rossiyskaya entsiklopediya, 1995, 928 p. (In Russ.)
4. Neganov V.A., Osipov O.V. *Reflective, Waveguide and Radiating Structures with Chiral Elements*. Moscow: Radio i svyaz', 2006, 280 p. (In Russ.)
5. Aralkin M.V., Dement'ev A.N., Osipov O.V. Mathematical models of chiral metamaterials based on multi-pass conducting elements. *Physics of Wave Processes and Radio Systems*, 2020, vol. 23, no. 1, pp. 8–19. DOI: https://doi.org/10.18469/1810-3189.2020.23.1.8-19 (In Russ.)
6. Osipov O.V., Pocheptsov A.O., Antipova T.A. Electrodynamics of planar reflective structures with chiral layers based on thin-wire spiral elements. *Physics of Wave Processes and Radio Systems*, 2018, vol. 21, no. 3, pp. 59–65. URL: https://journals.ssau.ru/pwp/article/view/7019 (In Russ.)
7. Yurtsev O.A., Runov A.V., Kazarin A.N. *Spiral Antennas*. Moscow: Sov. radio, 1974, 223 p. (In Russ.)
8. Mei K. On the integral equations of thin wire antennas. *IEEE Transactions on Antennas and Propagation*, 1965, vol. 13, no. 3, pp. 374–378. DOI: https://doi.org/10.1109/TAP.1965.1138432
9. Adekola S., Mowete A., Ayorinde A. Compact theory of the broadband elliptical helical antenna. *European Journal of Scientific Research*, 2009, vol. 31, no. 3, pp. 446–490.
10. Chebyshev V.V. *Microstrip Antennas in Multilayer Environments*. Moscow: Radiotekhnika, 2007, 160 p. (In Russ.)
11. Neganov V.A., Tabakov D.P. Mathematical models of a cylindrical helical antenna. *Physics of Wave Processes and Radio Systems*, 2013, vol. 16, no. 4, pp. 79–86. (In Russ.)
12. Strizhkov V.A. Mathematical modeling of electrodynamic processes in wire antenna systems. *Matematicheskoe modelirovanie*, 1989, vol. 1, no. 8, pp. 127–138. URL: https://www.mathnet.ru/rus/mm/v1/i8/p127 (In Russ.)
13. Neganov V.A. Integral representation of the electromagnetic field of a geometrically chiral structure. *Physics of Wave Processes and Radio Systems*, 2012, vol. 15, no. 4, pp. 6–13. (In Russ.)
14. Tabakov D.P. On the description of radiation and diffraction of electromagnetic waves by the method of eigenfunctions. *Izvestiya vuzov. Radiofizika*, 2021, vol. 64, no. 3, pp. 179–191. URL: https://radiophysics.unn.ru/issues/2021/3/179 (In Russ.)
15. Bakhvalov N.S., Zhidkov N.P., Kobel'kov G.M. *Numerical Methods*. Moscow: Binom; Laboratoriya znaniy, 2008, 686 p. (In Russ.)
16. Neganov V.A., Nefedov E.I., Yarovoy G.P. *Electrodynamic Methods for Designing Microwave Devices and Antennas*. Ed. by V.A. Neganov. Moscow: Radio i svyaz', 2002, 416 p. (In Russ.)
17. Tabakov D.P., Morozov S.V., Klyuev D.S. Application of the thin-wire integral representation of the electromagnetic field to the solution of the problem of diffraction of electromagnetic waves by conducting bodies. *Physics of Wave Processes and Radio Systems*, 2022, vol. 25, no. 2, pp. 7–14. DOI: https://doi.org/10.18469/1810-3189.2022.25.2.7-14 (In Russ.)

Список литературы

1. Рамсей В. Частотно-независимые антенны. М.: Мир, 1968. 176 с.
2. Драбкин А.Л., Зузенко В.Л., Кислов А.Г. Антенно-фидерные устройства. Изд. 2-е, доп. и перераб. М.: Сов. радио, 1974. 536 с.

3. Физический энциклопедический словарь / под ред. А.М. Прохорова. М.: Большая российская энциклопедия, 1995. 928 с.

4. Неганов В.А., Осипов О.В. Отражающие, волноведущие и излучающие структуры с киральными элементами. М.: Радио и связь, 2006. 280 с.

5. Аралкин М.В., Дементьев А.Н., Осипов О.В. Математические модели киральных метаматериалов на основе многозаходных проводящих элементов // Физика волновых процессов и радиотехнические системы. 2020. Т. 23, № 1. С. 8–19. DOI: https://doi.org/10.18469/1810-3189.2020.23.1.8-19

6. Осипов О.В., Почепцов А.О., Антипова Т.А. Электродинамика планарных отражающих структур с киральными слоями на основе тонкопроволочных спиральных элементов // Физика волновых процессов и радиотехнические системы. 2018. Т. 21, № 3. С. 59–65. URL: https://journals.ssau.ru/pwp/article/view/7019

7. Юрцев О.А., Рунов А.В., Казарин А.Н. Спиральные антенны. М.: Сов. радио, 1974. 223 с.

8. Mei K. On the integral equations of thin wire antennas // IEEE Transactions on Antennas and Propagation. 1965. Vol. 13, no. 3. P. 374–378. DOI: https://doi.org/10.1109/TAP.1965.1138432

9. Adekola S., Mowete A., Ayorinde A. Compact theory of the broadband elliptical helical antenna // European Journal of Scientific Research. 2009. Vol. 31, № 3. P. 446–490.

10. Чебышев В.В. Микрополосковые антенны в многослойных средах. М.: Радиотехника, 2007. 160 с.

11. Неганов В.А., Табаков Д.П. Математические модели цилиндрической спиральной антенны // Физика волновых процессов и радиотехнические системы. 2013. Т. 16, № 4. С. 79–86.

12. Стрижков В.А. Математическое моделирование электродинамических процессов в проволочных антенных системах // Математическое моделирование. 1989. Т. 1, № 8. С. 127–138. URL: https://www.mathnet.ru/rus/mm/v1/i8/p127

13. Неганов В.А. Интегральное представление электромагнитного поля геометрически киральной структуры // Физика волновых процессов и радиотехнические системы. 2012. Т. 15, № 4. С. 6–13.

14. Табаков Д.П. Об описании излучения и дифракции электромагнитных волн методом собственных функций // Известия вузов. Радиофизика. 2021. Т. 64, № 3. С. 179–191. URL: https://radiophysics.unn.ru/issues/2021/3/179

15. Бахвалов Н.С., Жидков Н.П., Кобельков Г.М. Численные методы. М.: Бином; Лаборатория знаний, 2008. 686 с.

16. Неганов В.А., Нефедов Е.И., Яровой Г.П. Электродинамические методы проектирования устройств СВЧ и антенн / под ред. В.А. Неганова. М.: Радио и связь, 2002. 416 с.

17. Табаков Д.П., Морозов С.В., Клюев Д.С. Применение тонкопроволочного интегрального представления электромагнитного поля к решению задачи дифракции электромагнитных волн на проводящих телах // Физика волновых процессов и радиотехнические системы. 2022. Т. 25, № 2. С. 7–14. DOI: https://doi.org/10.18469/1810-3189.2022.25.2.7-14

Физика волновых процессов и радиотехнические системы
2023. Т. 26, № 1. С. 38–48

DOI 10.18469/1810-3189.2023.26.1.38-48
УДК 537.862

Дата поступления 29 ноября 2022
Дата принятия 30 декабря 2022

Математические модели сфероидальных спирально-рамочных излучателей

Д.П. Табаков, Р.М. Валиуллин

Поволжский государственный университет телекоммуникаций и информатики
443010, Россия, г. Самара,
ул. Л. Толстого, 23

Аннотация – В статье рассмотрены математические модели двух сфероидальных спирально-рамочных излучателей, построенные на основе общего подхода, предполагающего использование интегрального представления электромагнитного поля. Построение моделей осуществлялось в тонкопроволочном приближении. Внутренняя задача электродинамики сведена к системе интегральных уравнений Фредгольма 1-го рода. Решение полученной системы осуществлялось методом моментов с кусочно-постоянными базисными функциями и дельта-функциями в качестве тестовых функций. При этом осуществлялась локальная линеаризация образующих проводников рассматриваемых структур. Проведены исследования зависимостей распределений токов, входного сопротивления и характеристик излучения структур от частоты. Показано, что в рассматриваемых структурах возможно существование стоячих, бегущих и смешанных волн тока. Режим тока определяется волновыми размерами и геометрией структур и определяет характер поведения волнового сопротивления в диапазоне частот. Несмотря на схожую геометрию, характеристики рассмотренных структур имеют определенные отличия.

Ключевые слова – спиральные антенны; рамочные антенны; интегральное представление электромагнитного поля; тонкопроволочное приближение; диаграмма направленности; входное сопротивление.

Information about the Authors

Dmitry P. Tabakov, Doctor of Physical and Mathematical Sciences, professor of the Department of Physics, Povolzhskiy State University of Telecommunications and Informatics, Samara, Russia.
Research interests: electrodynamics, microwave devices and antennas, optics, numerical methods of mathematical modeling.
E-mail: illuminator84@yandex.ru

Ruslan M. Valiullin, post-graduate student of the Department of Physics, Povolzhskiy State University of Telecommunications and Informatics, Samara, Russia.
Research interests: electrodynamics, microwave devices and antennas.
E-mail: ruslanvaliullin1998@yandex.ru

Информация об авторах

Табаков Дмитрий Петрович, доктор физико-математических наук, профессор кафедры физики Поволжского государственного университета телекоммуникаций и информатики, г. Самара, Россия.
Область научных интересов: электродинамика, устройства СВЧ и антенны, оптика, численные методы математического моделирования.
E-mail: illuminator84@yandex.ru

Валиуллин Руслан Миндарович, аспирант кафедры физики Поволжского государственного университета телекоммуникаций и информатики, г. Самара, Россия.
Область научных интересов: электродинамика, устройства СВЧ и антенны.
E-mail: ruslanvaliullin1998@yandex.ru